Current Biology 25, 69–74, January 5, 2015 ©2015 Elsevier Ltd All rights reserved http://dx.doi.org/10.1016/j.cub.2014.10.055

Report

A Spinal Opsin Controls Early Neural Activity and Drives a Behavioral Light Response

Drew Friedmann,[1] Adam Hoagland,[1] Shai Berlin,[1,2] and Ehud Y. Isacoff[1,2,3,*]

[1]Department of Molecular and Cell Biology, University of California, Berkeley, Berkeley, CA 94720, USA

[2]Helen Wills Neuroscience Institute, University of California Berkeley, Berkeley, CA 94720, USA

[3]Physical Bioscience Division, Lawrence Berkeley National Laboratory, Berkeley, CA 94720, USA

Summary

Nonvisual detection of light by the vertebrate hypothalamus, pineal, and retina is known to govern seasonal and circadian behaviors [1]. However, the expression of opsins in multiple other brain structures [2–4] suggests a more expansive repertoire for light regulation of physiology, behavior, and development. Translucent zebrafish embryos express extraretinal opsins early on [5, 6], at a time when spontaneous activity in the developing CNS plays a role in neuronal maturation and circuit formation [7]. Though the presence of extraretinal opsins is well documented, the function of direct photoreception by the CNS remains largely unknown. Here, we show that early activity in the zebrafish spinal central pattern generator (CPG) and the earliest locomotory behavior are dramatically inhibited by physiological levels of environmental light. We find that the photosensitivity of this circuit is conferred by vertebrate ancient long opsin A (VALopA), which we show to be a $G\alpha_i$-coupled receptor that is expressed in the neurons of the spinal network. Sustained photoactivation of VALopA not only suppresses spontaneous activity but also alters the maturation of time-locked correlated network patterns. These results uncover a novel role for nonvisual opsins and a mechanism for environmental regulation of spontaneous motor behavior and neural activity in a circuit previously thought to be governed only by intrinsic developmental programs.

Results and Discussion

During the development of the nervous system, the first incidence of neural activity often occurs before sensory experience [7]. The frequency and pattern of this spontaneously generated activity guide neuronal differentiation, axon pathfinding, and synapse formation in many species and brain regions, including retina [8, 9], cortex [10, 11], hippocampus [12, 13], and spinal cord [14–17]. Because these activity networks are robust and stereotyped, we were surprised to find that spontaneous behavior, exhibited by embryonic zebrafish during the formation of its spinal central pattern generator (CPG), is heavily regulated by an unexpected external stimulus: light. Coiling behavior (Figure 1A; Movie S1 available online), a prelocomotory behavior that is driven by spontaneous CPG activity [18, 19], was dramatically suppressed by illumination with green light (508 nm at 13.2 $\mu W/mm^2$) (Figure 1B). In dark-adapted fish at 22.5 hr postfertilization (hpf), coiling ceased within 1.7 ± 1.4 s of the start of illumination, and the suppression persisted during a 2 min period of constant illumination (Figures 1C and 1D, left). The light-induced suppression was also seen several hours later (27 hpf) but was preceded by a brief and transient phase of increased activity, as described recently [20] (Figure 1D, right). A systematic examination over early development revealed that photoinhibition is present as soon as motor activity begins (Figures 1E and S1A).

Coiling was suppressed by light over a broad range of wavelengths, with a behavioral response λ_{max} at 504 nm (Figure 1F) and was inhibited by flashes of light as short as 70 ms (Figures 1G and S1E). The suppression lasted long after the termination of a light pulse, recovering to baseline dark frequency over minutes ($t_{1/2}$ = 165 ± 21 s, n = 96) (Figure S1B). When illumination continued for minutes, the suppression of coiling partly adapted, relaxing to 43.0% ± 2.5% (n = 96) of the dark-adapted frequency (Figure S1C). Recovery from the light-adapted state also required minutes, similar to the recovery from a brief (2 s) light exposure (Figures S1C and S1D), demonstrating that the rate of recovery is independent of the extent of the inhibition and implying that the recovery from different light regimens engages similar signaling cascades. This also shows that the rapid freezing behavior is a genuine light-dependent response, rather than a nonspecific reaction to an abrupt contrast change, such as the reversion to darkness after light adaptation (Figure S1C).

At these early ages, zebrafish are blind because photoreceptors and retinal circuitry have not yet developed [21]. We therefore wondered whether the photoinhibition of coiling could reflect an intrinsic property of the CPG network. The nascent CPG resides entirely within the spinal cord, requiring putative pacemaker neurons in the most rostral somites, but not the hindbrain [22, 23]. We hypothesized that the calcium activity in the CPG network should therefore also be affected by light. Of the four earliest active cell types—ipsilateral-caudal projecting pacemakers (ICs), primary motor neurons (PMNs), ventral longitudinal descending interneurons (VeLDs), and sensory-driven contralaterally projecting ascending neurons (CoPAs)—the PMNs and VeLDs are contained within the 1020:Gal4 enhancer trap transgenic line [18, 22–26]. We used the genetically encoded calcium indicator GCaMP5 [27] to examine the effect of light on the activity of these cells (Figure 2A, left). To minimize potential photoinhibition during calcium imaging, we excited GCaMP5 with two-photon (2P) illumination at 920 nm. Under this condition, we observed spontaneous calcium events in 1020:$Gal4^+$ neurons at a frequency of 6.8 ± 0.7 events/min (n = 10 fish) (Figure 2A, black trace). The frequency was reduced by about half when excitation of GCaMP5 was switched to one-photon (1P) illumination at 488 nm (3.6 ± 0.5 events/min; n = 10 fish) (Figure 2A, gray trace). Akin to the photoinhibition of coiling behavior, neural activity at the end of the first day of development responded to a 5 s stimulus of 561 nm light with a sustained reduction in the frequency of calcium events (e.g., 24 hpf; Figures 2B and 2C), and the inhibition was also induced by the blue-green portion of the visible spectrum (Figure 2D). Interestingly,

*Correspondence: ehud@berkeley.edu

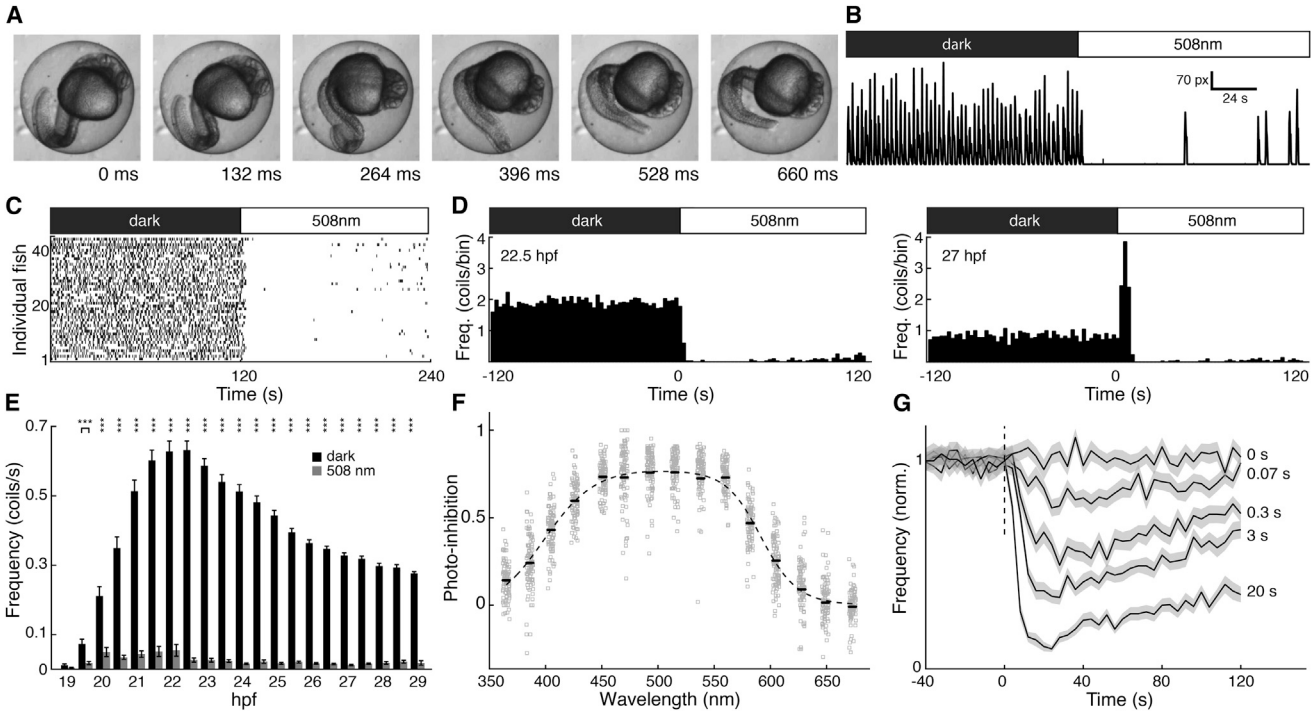

Figure 1. Effect of Light on Frequency of Spontaneous Coiling Behavior

(A) Still frames from a movie of a single spontaneous coil in a 27 hpf embryo.

(B) Trace of detected motion (pixel changes) from video of an individual embryo before (dark) and during (508 nm) illumination; peaks represent individual coiling events.

(C) Raster plot of coiling events measured simultaneously in 44 dark-adapted 22.5 hpf embryos under dark and light conditions.

(D) Left, peristimulus time histogram of 22.5 hpf embryos from data in (C). Right, histogram of the same fish at 27 hpf. Frequency is mean coils/fish within bins of 2.4 s.

(E) Mean (±SEM) baseline coiling frequencies (coils/s) in the dark (black bars) and under green light (gray bars) over developmental time. Two-tailed paired t test with Bonferroni adjusted p values, ***$p < 0.001$; n = 39–75.

(F) Photoinhibition [$-(Hz_{Light} - Hz_{Dark}) / Hz_{Dark}$; coiling measured over 120 s in each condition] as a function of wavelength. Gray squares are individual responses <3 SD from each mean (black lines). Light power = 133–159 nW/mm^2; n = 96.

(G) Photoinhibition of coiling frequency by light flashes of indicated durations. Lines indicate normalized mean, bins = 4 s; SEM in gray; n = 96.

See also Figure S1.

ipsilateral correlation and contralateral alternation were not affected (Figures 2B and S2A), suggesting that acute light stimulation slows, rather than disrupts, natural behavior.

Detectable photoinhibition of neural activity became evident at 20.5 hpf, shortly after activity in the network reaches its peak frequency (Figures 2C and S2B). As compared to photoinhibition of coiling, the effect on neural activity appeared later and of smaller magnitude (compare with Figures 1E and S1A). These differences may arise from the methodological difference between whole-animal illumination, used to study coiling, and very localized illumination, as is done in GCaMP experiments. During Ca^{2+} imaging, only somites 3–8 received the light stimulus—a fraction of the spinal cord, and missing the most mature, rostral portion of the spinal circuit. Nevertheless, the photoinhibition of neuronal activity by local illumination indicates that somites 3–8 of the spinal cord contain a light sensor that suppresses spontaneous activity.

Between 17 and 20 hpf, newly active neurons join into a circuit formed by ipsilaterally projecting interneurons and switch their pattern of activity from irregular, long, and isolated events to bursts of short events that are correlated among electrically coupled cells on the same side of the cord [18, 26]. By 22 hpf, most active 1020:Gal4$^+$ neurons have joined the CPG network, whereas a small group of cells display long duration and uncorrelated activity [17, 26]. Previously, inhibition of early activity was shown to increase the fraction of the uncorrelated cells with long calcium events [26]. We found here that inhibiting activity before 20 hpf via global illumination with green light similarly resulted in a significantly higher percentage of active cells with long-duration, noncorrelated calcium events at 22 hpf (Figure 2E, dashed area).

In an effort to identify genes whose protein products are involved in inhibition of the spinal CPG, we used fluorescence-activated cell sorting (FACS) to purify fluorescent protein-expressing cells labeled by the UAS promoter when crossed to 1020:Gal4$^+$ fish (Figure S3A). Cells from trunk and tail samples of 20 hpf reporter fish were isolated, total RNA was extracted, and RNA sequencing analysis was performed [28]. We compared gene expression levels from the 1020:Gal4$^+$ subpopulation of neurons to those labeled in the pan-neuronal HuC:Gal4 line. Among the transcripts whose expression was elevated in 1020:Gal4$^+$ neurons was *valopa* (vertebrate ancient long opsin A; VALopA), an extraretinal photoreceptor and evolutionary intermediate between invertebrate opsins and vertebrate visual photoreceptors [29]. Other genes with elevated expression in 1020:Gal4$^+$ neurons included known ventral spinal cord and motor neuron markers, as well as *olig2*, the genomic insertion site of the 1020:Gal4

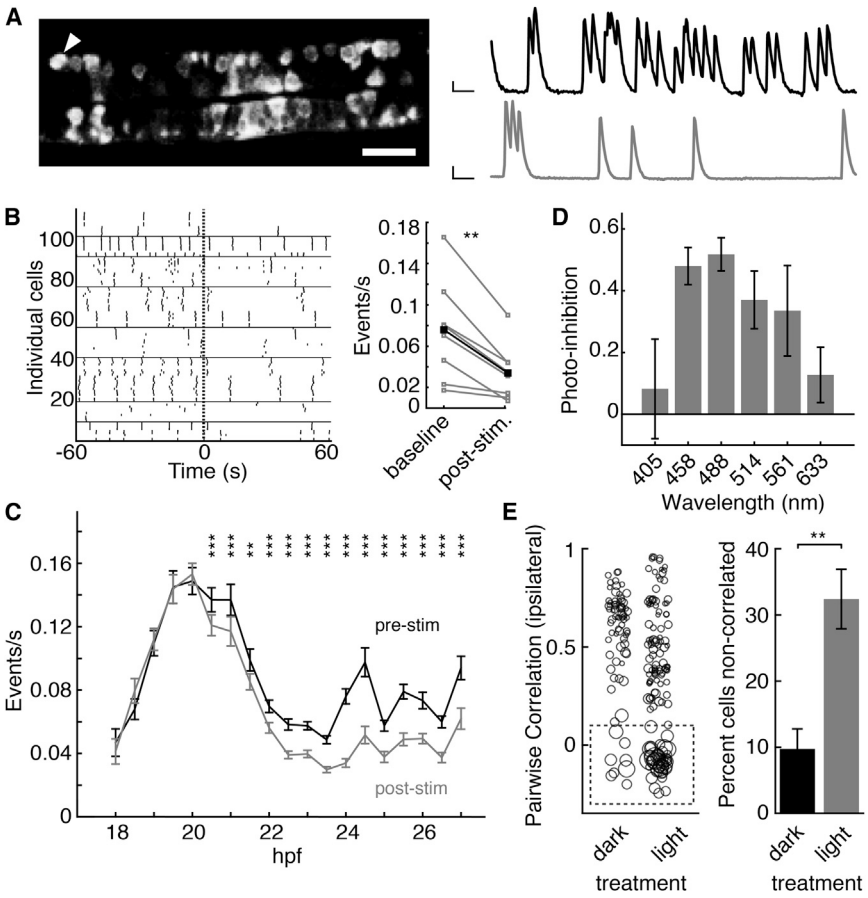

Figure 2. Acute and Delayed Effects of Light on Neural Activity

(A) Left, image of GCaMP5 fluorescence in ventral spinal cord somites 3–8 of a 1020:Gal4; UAS: GCaMP5 embryo. Scale bar, 20 μm. Right, calcium traces from one cell (arrowhead in image) under 2P (black trace, 920 nm) or subsequent period of 1P (gray trace, 488 nm) excitation, after <5 s interval. Axes: 100% ΔF/F, 10 s.

(B) Left, raster plot of 2P-imaged calcium events in 24 hpf embryos before and after a 5 s flash (dashed line) with 561 nm light. Measurements from each of eight fish (horizontal lines delineate individual fish). Right, quantification of calcium event frequency in the eight fish (gray lines; black line, mean) during a 180 s period under 2P excitation (baseline) and over 60 s after the 561 nm light flash (post-stim). Two-tailed paired t test $p < 0.01$.

(C) Frequency (mean ± SEM) of calcium events over 9 hr of development measured under 2P excitation before (pre-stim) and after (post-stim) a 5 s 561 nm light flash, as quantified in (B). Two-tailed paired t test, Bonferroni adjusted p values, ***$p < 0.001$, **$p < 0.01$; n = 21–123 cells from four to eight fish at each age.

(D) Photoinhibition (mean ± SEM) after illumination with a 5 s light flash at varying wavelengths. 103–110 μW/pixel; n = 16 cells in eight fish at each wavelength.

(E) Left, pairwise ipsilateral correlations between cells in 22 hpf embryos after dark or light (508 nm, 13.2 μW/mm^2) rearing for 2 hr before 20 hpf. Circle size proportional to event width at half max amplitude (range = 1.8–75.7 s). Dashed box demarcates noncorrelated cells. Right, percentage (±SEM) of noncorrelated cells (ipsilateral correlation <0.1) at 22 hpf. Two-tailed unpaired t test, $p = 0.004$. n = 6 (dark) and n = 8 (light) fish.

See also Figure S2.

enhancer trap [25] (Figures S3B and S3C). VALopA appeared to be a good candidate photoreceptor for inhibition of the spinal CPG based on its known presence in the spinal cord at 24 hpf and its previously described absorbance spectrum (λ_{max} = 510 nm) [5].

To test the hypothesis that VALopA is the photoreceptor mediating spinal CPG photoinhibition, we used morpholino knockdown of VALopA expression [20]. The morpholino for VALopA, but not the scrambled control, completely abolished the inhibitory photoresponse in both young and older fish (Figures 3A–3C; Movie S2). At later ages, when transient photoexcitation preceded photoinhibition (Figure 3D), VALopA knockdown selectively abrogated the sustained photoinhibition (Figure 3B). Thus, photoinhibition develops concurrently with coiling, is elicited by spinal illumination alone, and requires VALopA. Conversely, photoexcitation develops later, is elicited by hindbrain illumination, and is independent of VALopA, in agreement with a recent report [20]. In order to determine whether photoactivation of VALopA in 1020:Gal4$^+$ neurons is sufficient to drive inhibition, we mosaically expressed UAS-VALopA with a cerulean fluorescent marker in 1020:Gal4$^+$ fish whose VALopA expression was knocked down by the splice-blocking morpholino. Photoinhibition was seen only when the rescue construct was broadly expressed, and the degree of photoinhibition increased with the expression level of the mCerulean marker, reporting higher expression levels of VALopA (Figures 3E and 3F).

To better understand the mechanism of photoinhibition, we attempted to identify the intracellular signaling pathway that is activated by VALopA. We heterologously expressed zebrafish VALopA in *Xenopus laevis* oocytes and performed two-electrode voltage clamp recordings. Oocytes had no native light response, nor did injection of cRNA encoding VALopA on its own introduce a detectable light response (Figure 4A). However, coinjection of cRNAs encoding VALopA$_{GFP}$ and the neuronal G protein activated inward rectifying potassium (GIRK) channel subunits (GIRK1$_{mCherry}$/GIRK2) (Figure S4A), yielded a large photocurrent. Increasing external [K$^+$] from 2 to 24 mM generated an inward current (Figures 4A and 4B), as is typical of basal activation of GIRK by free native Gβγ in the oocyte [30]. Illumination with 535 nm light evoked an additional increase in current amplitude above basal level (Figures 4A, 4B, and S4B), as is observed with ligand activation of the Gα$_i$ class of G-protein-coupled receptors (GPCRs), such as the acetylcholine-activated muscarinic-2 receptor m2R [31] (Figures S4D–S4F). Unlike activation of other GPCRs, the combined current persisted without decay for tens of seconds after the light was turned off (Figures 4A and S4B). Inward currents were blocked by the GIRK-channel blocker Ba^{2+}, further confirming that the light-induced currents are GIRK mediated. These data suggest that VALopA is a Gα$_i$-coupled GPCR that turns off very slowly. In support of this, the photocurrent was inhibited by expression of the specific Gα$_i$-inactivating pertussis toxin (PTX), even when coexpressed with additional wild-type Gα$_{i3}$ (Figures 4C and 4D). Moreover, PTX-insensitive Gα$_{i3}$ (C351I) [32] faithfully restored the photocurrent in the presence of PTX (Figures 4C and 4D). As observed with the suppression of coiling behavior in zebrafish, GIRK current in

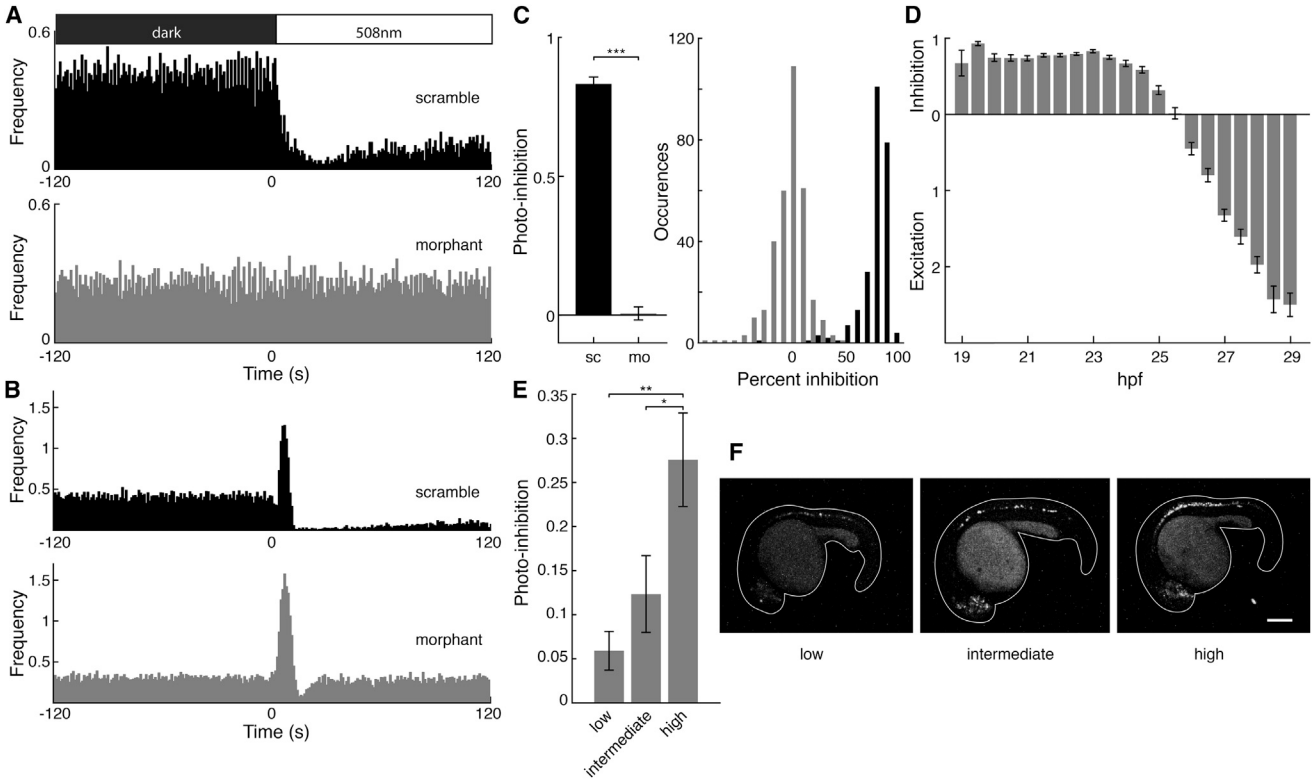

Figure 3. Light Inhibition of Coiling Depends on an Extraretinal Opsin

(A and B) Representative peristimulus time histograms of coiling frequency (events/s; mean across six trials; bin = 1 s) of embryos at 22–25 hpf (A) or 27–31 hpf (B). Zygotes injected with scrambled control morpholino (n = 23 in A, 34 in B) (black) or morpholino against VALopA (n = 24 in A, 41 in B) (gray).

(C) Left, mean photoinhibition (±SEM) of scrambled control morpholino (sc; n = 40) and morpholino (mo; n = 55) -injected 22–25 hpf embryos. Two-tailed unpaired t test, $p < 0.001$. Right, frequency distribution of percent photoinhibition (six responses per fish) in scrambled control morpholino embryos (black) and morpholino embryos (gray).

(D) Normalized inhibition or excitation (mean ± SEM) of coiling frequency [− (Hz_{Light} − Hz_{Dark}) / Hz_{Dark}] in the first 12 s after light onset relative to a 120 s preceding baseline in darkness (n = 39–75).

(E) Mean photoinhibition (±SEM; five responses per fish) of morpholino-injected embryos mosaically expressing low, intermediate, or high levels of a VALopA rescue construct with a mCerulean marker. One-way ANOVA with Tukey post hoc analysis, *$p < 0.05$, **$p < 0.01$; n = 59 (low), 18 (intermediate), and 11 (high).

(F) Images of representative embryos expressing low, intermediate, and high levels of mCerulean fluorescence. Scale bar, 200 μm.

See also Figure S3.

oocytes could be triggered by very brief flashes of light (as short as 5 ms) and, as mentioned above, persisted for minutes afterward in the dark (Figure S4C). Together, these findings indicate that VALopA couples to the $G\alpha_i$ pathway and suggest that the slow kinetics of this signaling can explain the kinetics of the light-induced inhibition of spontaneous activity and behavior in zebrafish.

Early optogenetics experiments demonstrated the ability of rat rhodopsin to couple to $G\alpha_i$ and inhibit spontaneously active networks in chick spinal cord [33]. We show that, in fish, VALopA photoinhibition similarly influences early activity before the onset of touch, sound, or visual responses, making it the earliest sensory input to the zebrafish spinal cord. At these early ages, spontaneous activity is an important developmental determinant before circuits, synapses, and cell fates are finalized [14–16, 26, 34, 35]. Whereas some activity-dependent processes require competition between neurons, global activity levels were recently shown to regulate transmitter fate in *Xenopus* through the regulation of secreted brain-derived neurotrophic factor [35]. Indeed, we find that global photoinhibition in early zebrafish affects the distribution of subsequent activity patterns in the locomotory CPG, perhaps reflecting a mechanism by which the light-dark cycle can sculpt early development. It is also conceivable, by analogy to the function of a VALopA homolog in ascidian larvae [36, 37] and a nonvisual photoreceptor in *Drosophila* larvae [38], that VALopA mediates a photosensitive avoidance behavior. At sunrise in the wild, embryos will be at varying stages of development, depending on spawning time and water temperature [39, 40]. The consistent inhibition by VALopA across these ages could drive a freezing behavior in bright light that eludes predators at a time when the embryo is trapped in the chorion and before sensory-evoked escape behavior emerges. The uneven timing of development and sunrise could also affect activity-driven processes in an age-dependent fashion, but it is unknown whether this would diversify or synchronize the relationship between development and the photoperiod. It will be interesting to see whether spontaneously active circuits in other brain regions are similarly flexible to environmental regulation and also whether nonvisual opsins can acutely control behavior in other vertebrates.

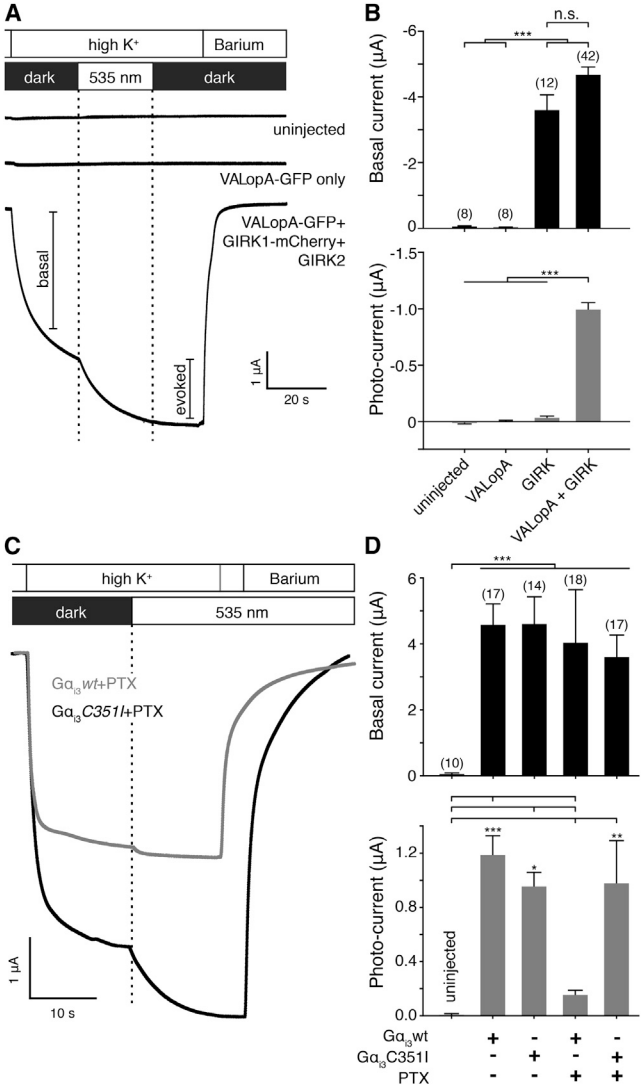

Figure 4. VALopA Couples to $Ga_{i/o}$ in *Xenopus* Oocytes

(A) Representative voltage clamp currents from an uninjected oocyte (top trace), an oocyte expressing zebrafish $VALopA_{GFP}$ alone (middle trace) or coexpressing $VALopA_{GFP}$ with $GIRK1_{mCherry}$ and GIRK2. Oocytes are initially bathed in ND96 and switched to 24 mM K^+ (high K^+) and then 5 mM Ba^{2+} in 24 mM K^+ (Barium). Illumination through a 535/50 nm bandpass filter (~70 mW/mm^2) is indicated.

(B) Summary for the basal (top) and light-evoked (bottom) GIRK currents as in (A).

(C) Representative currents (protocols as in A) from oocytes expressing $VALopA_{GFP}$, $GIRK1_{mCherry}$ and GIRK2 with the catalytic subunit of pertussis toxin (PTX-S1) and either PTX-sensitive $G\alpha_{i3}$-*wt* (gray) or PTX-insensitive C351I mutant $G\alpha_{i3}$ (black).

(D) Summary for the basal (top) and light-evoked (bottom) GIRK currents in oocytes expressing combinations of $G\alpha_{i3}$-*wt*, $G\alpha_{i3}$-C351I, and PTX. One-way ANOVA with Tukey post hoc analysis *p < 0.05, **p < 0.01, ***p < 0.001; n is indicated above bars; error bars represent SEM.

See also Figure S4.

Experimental Procedures

Zebrafish Behavior and Calcium Imaging

Behavioral tests characterizing photoinhibition were conducted between 22 and 25 hpf with additional experiments from 19 to 31 hpf. All wild-type *Danio rerio* were from the AB strain, and all animal care and experiments were in accordance with the University of California at Berkeley Animal Care and Use Committee guidelines. Transgenic UAS:GCaMP5 fish were generated using Tol2 transposase and subsequently crossed to the *Gal4s1020t* driver line. Two-photon movies were acquired using 920 nm for visualizing GCaMP5 fluorescence. Light stimulation consisted of scans across the imaging area with laser light in the visible spectrum.

FACS Sequencing

In brief, tails were dissected from groups of fish expressing fluorescent markers within the 1020:Gal4 or panneuronal HuC:Gal4 cell populations. Dissociated tails were sorted to isolate pools of labeled neurons before RNA was extracted for library generation and sequencing.

Oocyte Physiology

mRNAs for VALopA, GIRK1/2, $G\alpha_{i3}$, m2R, and PTX were injected into oocytes and incubated for 3–4 days for expression. Whole-cell currents were measured using standard two-electrode voltage clamp procedures.

Accession Numbers

RNA-seq .fastq files can be found via the Gene Expression Omnibus archive under accession number GSE62527.

Supplemental Information

Supplemental Information includes Supplemental Experimental Procedures, four figures, and two movies and can be found with this article online at http://dx.doi.org/10.1016/j.cub.2014.10.055.

Author Contributions

D.F. conceived the project. D.F. and E.Y.I. designed the experiments. Oocyte recordings and analysis were performed by S.B. Hardware and software were built and written by A.H. All other experiments were performed and analyzed by D.F. The manuscript was written by D.F. and E.Y.I. with input from S.B.

Acknowledgments

We thank H. Nolla and the Berkeley Flow Cytometry Core for assistance with FACS, Y.G. Choi, J. Ngai, and the Berkeley Functional Genomics Laboratory for assistance and guidance with RNA-seq. This work used the Vincent J. Coates Genomics Sequencing Laboratory at UC Berkeley, supported by NIH S10 Instrumentation Grants S10RR029668 and S10RR027303. We also thank D. Kojima (University of Tokyo, Japan) for providing VALopA cDNA, N. Dascal (Tel Aviv University, Israel) for providing GIRK1, GIRK2, and $G\alpha_{i3}$, E. Reuveny (Weizmann Institute, Israel) for providing PTX-S1, and L. Looger (Janelia Farm) for making GCaMP5 available. This work was supported by the NIH Nanomedicine Development Center for the Optical Control of Biological Function (2PN2EY01824) and the Human Frontier Science Program (RGP0013/2010).

Received: September 15, 2014
Revised: October 21, 2014
Accepted: October 23, 2014
Published: December 4, 2014

References

1. Peirson, S.N., Halford, S., and Foster, R.G. (2009). The evolution of irradiance detection: melanopsin and the non-visual opsins. Philos. Trans. R. Soc. Lond. B Biol. Sci. *364*, 2849–2865.
2. Fernandes, A.M., Fero, K., Driever, W., and Burgess, H.A. (2013). Enlightening the brain: linking deep brain photoreception with behavior and physiology. BioEssays *35*, 775–779.
3. Cheng, N., Tsunenari, T., and Yau, K.-W. (2009). Intrinsic light response of retinal horizontal cells of teleosts. Nature *460*, 899–903.
4. Nissilä, J., Mänttäri, S., Särkioja, T., Tuominen, H., Takala, T., Timonen, M., and Saarela, S. (2012). Encephalopsin (OPN3) protein abundance in the adult mouse brain. J. Comp. Physiol. A Neuroethol. Sens. Neural Behav. Physiol. *198*, 833–839.
5. Kojima, D., Torii, M., Fukada, Y., and Dowling, J.E. (2008). Differential expression of duplicated VAL-opsin genes in the developing zebrafish. J. Neurochem. *104*, 1364–1371.

6. Fernandes, A.M., Fero, K., Arrenberg, A.B., Bergeron, S.A., Driever, W., and Burgess, H.A. (2012). Deep brain photoreceptors control light-seeking behavior in zebrafish larvae. Curr. Biol. *22*, 2042–2047.
7. Kirkby, L.A., Sack, G.S., Firl, A., and Feller, M.B. (2013). A role for correlated spontaneous activity in the assembly of neural circuits. Neuron *80*, 1129–1144.
8. Ackman, J.B., Burbridge, T.J., and Crair, M.C. (2012). Retinal waves coordinate patterned activity throughout the developing visual system. Nature *490*, 219–225.
9. Penn, A.A., Riquelme, P.A., Feller, M.B., and Shatz, C.J. (1998). Competition in retinogeniculate patterning driven by spontaneous activity. Science *279*, 2108–2112.
10. Garaschuk, O., Linn, J., Eilers, J., and Konnerth, A. (2000). Large-scale oscillatory calcium waves in the immature cortex. Nat. Neurosci. *3*, 452–459.
11. Yu, Y.-C., He, S., Chen, S., Fu, Y., Brown, K.N., Yao, X.-H., Ma, J., Gao, K.P., Sosinsky, G.E., Huang, K., and Shi, S.H. (2012). Preferential electrical coupling regulates neocortical lineage-dependent microcircuit assembly. Nature *486*, 113–117.
12. Kleindienst, T., Winnubst, J., Roth-Alpermann, C., Bonhoeffer, T., and Lohmann, C. (2011). Activity-dependent clustering of functional synaptic inputs on developing hippocampal dendrites. Neuron *72*, 1012–1024.
13. Ben-Ari, Y., Cherubini, E., Corradetti, R., and Gaiarsa, J.L. (1989). Giant synaptic potentials in immature rat CA3 hippocampal neurones. J. Physiol. *416*, 303–325.
14. Kastanenka, K.V., and Landmesser, L.T. (2010). In vivo activation of channelrhodopsin-2 reveals that normal patterns of spontaneous activity are required for motoneuron guidance and maintenance of guidance molecules. J. Neurosci. *30*, 10575–10585.
15. Plazas, P.V., Nicol, X., and Spitzer, N.C. (2013). Activity-dependent competition regulates motor neuron axon pathfinding via PlexinA3. Proc. Natl. Acad. Sci. USA *110*, 1524–1529.
16. Pineda, R.H., Svoboda, K.R., Wright, M.A., Taylor, A.D., Novak, A.E., Gamse, J.T., Eisen, J.S., and Ribera, A.B. (2006). Knockdown of Nav1.6a Na+ channels affects zebrafish motoneuron development. Development *133*, 3827–3836.
17. Gu, X., Olson, E.C., and Spitzer, N.C. (1994). Spontaneous neuronal calcium spikes and waves during early differentiation. J. Neurosci. *14*, 6325–6335.
18. Saint-Amant, L., and Drapeau, P. (2001). Synchronization of an embryonic network of identified spinal interneurons solely by electrical coupling. Neuron *31*, 1035–1046.
19. Saint-Amant, L. (2010). Development of motor rhythms in zebrafish embryos. Prog. Brain Res. *187*, 47–61.
20. Kokel, D., Dunn, T.W., Ahrens, M.B., Alshut, R., Cheung, C.Y.J., Saint-Amant, L., Bruni, G., Mateus, R., van Ham, T.J., Shiraki, T., et al. (2013). Identification of nonvisual photomotor response cells in the vertebrate hindbrain. J. Neurosci. *33*, 3834–3843.
21. Chhetri, J., Jacobson, G., and Gueven, N. (2014). Zebrafish—on the move towards ophthalmological research. Eye (Lond.) *28*, 367–380.
22. Pietri, T., Manalo, E., Ryan, J., Saint-Amant, L., and Washbourne, P. (2009). Glutamate drives the touch response through a rostral loop in the spinal cord of zebrafish embryos. Dev. Neurobiol. *69*, 780–795.
23. Tong, H., and McDearmid, J.R. (2012). Pacemaker and plateau potentials shape output of a developing locomotor network. Curr. Biol. *22*, 2285–2293.
24. Scott, E.K., Mason, L., Arrenberg, A.B., Ziv, L., Gosse, N.J., Xiao, T., Chi, N.C., Asakawa, K., Kawakami, K., and Baier, H. (2007). Targeting neural circuitry in zebrafish using GAL4 enhancer trapping. Nat. Methods *4*, 323–326.
25. Wyart, C., Del Bene, F., Warp, E., Scott, E.K., Trauner, D., Baier, H., and Isacoff, E.Y. (2009). Optogenetic dissection of a behavioural module in the vertebrate spinal cord. Nature *461*, 407–410.
26. Warp, E., Agarwal, G., Wyart, C., Friedmann, D., Oldfield, C.S., Conner, A., Del Bene, F., Arrenberg, A.B., Baier, H., and Isacoff, E.Y. (2012). Emergence of patterned activity in the developing zebrafish spinal cord. Curr. Biol. *22*, 93–102.
27. Akerboom, J., Chen, T.-W., Wardill, T.J., Tian, L., Marvin, J.S., Mutlu, S., Calderón, N.C., Esposti, F., Borghuis, B.G., Sun, X.R., et al. (2012). Optimization of a GCaMP calcium indicator for neural activity imaging. J. Neurosci. *32*, 13819–13840.
28. Ferreira, T., Wilson, S.R., Choi, Y.G., Risso, D., Dudoit, S., Speed, T.P., and Ngai, J. (2014). Silencing of odorant receptor genes by G protein $\beta\gamma$ signaling ensures the expression of one odorant receptor per olfactory sensory neuron. Neuron *81*, 847–859.
29. Sato, K., Yamashita, T., Ohuchi, H., and Shichida, Y. (2011). Vertebrate ancient-long opsin has molecular properties intermediate between those of vertebrate and invertebrate visual pigments. Biochemistry *50*, 10484–10490.
30. Reuveny, E., Slesinger, P.A., Inglese, J., Morales, J.M., Iñiguez-Lluhi, J.A., Lefkowitz, R.J., Bourne, H.R., Jan, Y.N., and Jan, L.Y. (1994). Activation of the cloned muscarinic potassium channel by G protein beta gamma subunits. Nature *370*, 143–146.
31. Lüscher, C., and Slesinger, P.A. (2010). Emerging roles for G protein-gated inwardly rectifying potassium (GIRK) channels in health and disease. Nat. Rev. Neurosci. *11*, 301–315.
32. West, R.E., Jr., Moss, J., Vaughan, M., Liu, T., and Liu, T.Y. (1985). Pertussis toxin-catalyzed ADP-ribosylation of transducin. Cysteine 347 is the ADP-ribose acceptor site. J. Biol. Chem. *260*, 14428–14430.
33. Li, X., Gutierrez, D.V., Hanson, M.G., Han, J., Mark, M.D., Chiel, H., Hegemann, P., Landmesser, L.T., and Herlitze, S. (2005). Fast noninvasive activation and inhibition of neural and network activity by vertebrate rhodopsin and green algae channelrhodopsin. Proc. Natl. Acad. Sci. USA *102*, 17816–17821.
34. Crisp, S.J., Evers, J.F., and Bate, M. (2011). Endogenous patterns of activity are required for the maturation of a motor network. J. Neurosci. *31*, 10445–10450.
35. Guemez-Gamboa, A., Xu, L., Meng, D., and Spitzer, N.C. (2014). Non-cell-autonomous mechanism of activity-dependent neurotransmitter switching. Neuron *82*, 1004–1016.
36. Kusakabe, T., Kusakabe, R., Kawakami, I., Satou, Y., Satoh, N., and Tsuda, M. (2001). Ci-opsin1, a vertebrate-type opsin gene, expressed in the larval ocellus of the ascidian Ciona intestinalis. FEBS Lett. *506*, 69–72.
37. Inada, K., Horie, T., Kusakabe, T., and Tsuda, M. (2003). Targeted knockdown of an opsin gene inhibits the swimming behaviour photoresponse of ascidian larvae. Neurosci. Lett. *347*, 167–170.
38. Xiang, Y., Yuan, Q., Vogt, N., Looger, L.L., Jan, L.Y., and Jan, Y.N. (2010). Light-avoidance-mediating photoreceptors tile the Drosophila larval body wall. Nature *468*, 921–926.
39. Spence, R., Ashton, R., and Smith, C. (2007). Oviposition decisions are mediated by spawning site quality in wild and domesticated zebrafish, Danio rerio. Behaviour *144*, 953–966.
40. Engeszer, R.E., Patterson, L.B., Rao, A.A., and Parichy, D.M. (2007). Zebrafish in the wild: a review of natural history and new notes from the field. Zebrafish *4*, 21–40.